J Neurophysiol 90: 675–682, 2003;
10.1152/jn.00331.2003.

Functional Organization of Parietal Neuronal Responses to Optic-Flow Stimuli

Hugo Merchant,[1,2] Alexandra Battaglia-Mayer,[1,2] and Apostolos P. Georgopoulos[1–5]

[1]*Brain Sciences Center, Veterans Affairs Medical Center 55417; and Departments of* [2]*Neuroscience,* [3]*Neurology and* [4]*Psychiatry, University of Minnesota Medical School and* [5]*Cognitive Sciences Center, University of Minnesota, Minneapolis, Minnesota 55455*

Submitted 4 April 2003; accepted in final form 21 April 2003

Merchant, Hugo, Alexandra Battaglia-Mayer, and Apostolos P. Georgopoulos. Functional organization of parietal neuronal responses to optic-flow stimuli. *J Neurophysiol* 90: 675–682, 2003; 10.1152/jn.00331.2003. We analyzed the dissimilarity matrix of neuronal responses to moving visual stimuli using tree clustering and multidimensional scaling (MDS). Single-cell activity was recorded in area 7a while random dots moving coherently in eight different kinds of motion (right-, left-, up-, and downward, clockwise, counterclockwise, expansion, contraction) were presented to behaving monkeys with eyes fixated. Tree clustering analyses showed that the {rightward, leftward}, {upward, downward}, and {clockwise, counterclockwise]} motions were clustered in three separate branches (i.e., horizontal, vertical, and rotatory motion, respectively). In contrast, expansion was in a lone branch, whereas contraction was also separate but within a larger cluster. The distances among these clusters were then subjected to an MDS analysis to identify the dimensions underlying the tree clustering observed. This analysis revealed two major factors in operation. The first factor separated expansion from all other stimulus motions, which seems to reflect the prominence of expansion during the common activity of locomotion. In contrast, the second factor separated planar motions from motion in depth, which suggests that the latter may hold a special place in visual motion processing.

INTRODUCTION

Visual motion in general is a pervasive stimulus in everyday life because it occurs when an organism is moving in the environment and/or when an object is moving within the visual field, both very common occurrences. Accordingly, visual motion is a powerful stimulus for activating a number of brain areas. Neurophysiological studies in animals (Andersen 1997; Boussaoud et al. 1990; Newsome et al. 1990) and functional neuroimaging studies in human subjects (Cheng et al. 1995; Tootell et al. 1995; Zeki et al. 1991) have documented the involvement of several areas in stimulus motion processing, including the middle temporal area (MT) (Albright 1984; Zeki 1974), medial superior temporal area (MST) (Tanaka et al. 1986; Van Essen et al. 1981), superior temporal polysensory area (Bruce et al. 1981; Oram et al. 1993), area 7a (Motter and Mountcastle 1981; Siegel and Read 1997; Merchant et al. 2001), and the ventral intraparietal area (Colbi et al. 1993). More detailed analyses of the neural mechanisms underlying visual motion processing have been performed in animal experiments the results of which indicate that different areas relate to different aspects of this processing. For example, cell responses in MT relate mostly to rectilinear motion for which a columnar arrangement is present (Zeki 1974). Indeed, the coherent engagement of neuronal populations in area MT using intracortical microstimulation has been found to bias the perception of stimulus motion in the direction of the preferred direction of the columns stimulated (Salzman et al. 1990, 1992). In addition to responding to rectilinear motion, cells in MST and area 7a also respond to optic-flow stimuli, including stimulus motion in depth (Duffy and Wurtz 1991; Merchant et al. 2001; Siegel and Read 1997; Tanaka and Saito 1989). Finally, the population vector analysis has been successfully applied in several studies to reconstruct the course of a moving visual stimulus from the discharge of cell ensembles in MT (Kruse et al. 2002), MST (Page and Duffy 1999), and area 7a (Steinmetz et al. 1987).

Optic flow corresponds to the changes in the optic array induced by the relative motion between the subject and the environment. Information about optic flow is indispensable for encoding direction of heading, orientation, and visual navigation in three-dimensional space, controlling posture and locomotion, and perception of moving objects and the selection of motor actions that allow the appropriate interaction with them (Koenderink 1986; Lee 1976, 1980). Neurons in area MST respond selectively to expansion, rotation, and deformation but also to mixtures of motions (plano-radial, -circular, etc.) (Duffy and Wurtz 1991; Lagae et al. 1994; Tanaka and Saito 1989; Tanaka et al. 1986). MST is reciprocally connected with parietal area 7a (Andersen 1990; Cavada and Goldman-Rakic 1989), which in turn also contains neurons with optic-flow selectivity (Merchant et al. 2001; Siegel and Read 1997). Area 7a not only elaborates on the processing of optic-flow information but also integrates optic flow with gaze-position signals (Read and Siegel 1997). In a recent study, we described the responses of single cells in area 7a to eight stimulus motions that covered all basic motions of optic-flow stimuli, namely right-, left-, up-, and downward, expansion, contraction, clockwise, counterclockwise stimulus motions (Merchant et al. 2001). In the present study, we investigated the functional organization of these responses using tree clustering and multidimensional scaling (MDS). Specifically, we sought to find out whether these responses in a neuronal ensemble are clus-

Address for reprint requests: Corresponding author: Apostolos P. Georgopoulos, Brain Sciences Center, One Veterans Drive, Minneapolis, MN, 55417. Tel: 612-725-2282, Fax: 612-725-2291, E-mail: omega@umn.edu

The costs of publication of this article were defrayed in part by the payment of page charges. The article must therefore be hereby marked "*advertisement*" in accordance with 18 U.S.C. Section 1734 solely to indicate this fact.

tered and, if so, to determine the superordinate dimensions underlying the resulting clusters. In these analyses we followed R. N. Shepard's pioneering approach in analyzing psychophysical measurements of similarity using tree clustering and MDS (Shepard 1980).

METHODS

Animals

Two male monkeys (*Macaca mulatta*, 6 and 7 kg body wt) were used in this study. Animal care conformed to the principles outlined in *The Guide for Care and Use of Laboratory Animals* (National Institutes for Health Publication No. 85-23, revised 1985). Animal studies protocols were approved by the local institutional review boards.

Visual stimuli

Stimuli were presented on a 69 × 69-cm tangent screen placed 48.5 cm in front of the animal. Small square patches of random dots were presented successively at 25 different positions in a regular 5 × 5 grid. The dots could move in eight different motion conditions: the four cardinal directions of translation (rightward, leftward, upward, downward), expansion, contraction, clockwise (CW) rotation, and counterclockwise (CCW) rotation. Stimuli were back-projected on the screen using an LCD projector (NEC Multisync MT 820/1020) with a refresh rate of 60 Hz. The whole screen subtended 71° of visual angle (DVA), at eye level. The small square patches were 13.8 × 13.8 cm and subtended 16.2 DVA on a side at the center of the screen. Stimuli were presented within such a patch for 400 ms, one patch at a time, with an inter-patch presentation interval of 150 ms. The stimuli were composed of 30 white dots moving within a square on a black background. Each dot was a circle of 0.35 DVA in diameter and moved for a maximum lifetime of 400 ms, after which it was assigned to a new random location within a square patch. If a moving dot traveled outside the patch displayed, it was relocated to a new random location within the square. The dots were relocated asynchronously to avoid coherent flickering of the stimuli. This constant reshuffling essentially eliminated pattern and density artifacts because the pattern of dots was changing constantly and each region within the square had approximately the same number of points at any time. The linear (constant) speed in the four directions of translation (left-, right-, up-, and downward), and mean linear speed in the directions of expansion and contraction was 40 DVA/s; the angular speed in both directions of rotation was 430°/s.

Task

The monkeys (*monkeys 1* and *2*) were seated in a primate chair with the left arm loosely restrained. In the visual stimulation task, a yellow spot of 0.32 DVA diameter served as the fixation point (FP) and was presented in the center of the translucent tangent screen. The monkeys were trained to fixate this spot (within 2 DVA) for the duration of stimulus presentation. During that time, *monkey 1* maintained the right hand in a relaxed position (monitored using a video camera), whereas *monkey 2* maintained grasp of a vertical semi-isometric joystick with the right hand by exerting a constant pulling force on the joystick of ~0.22 N. First, the FP was turned on which the monkeys fixated; following attainment of fixation, 100–500 ms were allowed for *monkey 2* to grasp the joystick. Then stimuli were presented on the screen. A juice reward was delivered randomly every 1.1–3.3 s while fixation was maintained; if fixation was broken, the trial was aborted. The *x-y* eye position was monitored using an oculometer (Dr. Bouis, Karlsruhe, Germany). Both the eye and the joystick position were sampled at 200 Hz. The eight different motion conditions were interleaved and presented in a pseudorandom order. The 25 different patch locations were nested within each stimulus motion condition and were also presented pseudorandomly. A complete run consisted of the presentation of all conditions in three repetitions.

Neural recordings

Impulse activity of single neurons was recorded extracellularly from area 7a (left hemisphere). The recording sites have been published elsewhere (Merchant et al. 2001). All isolated neuronal potentials were recorded regardless of their activity during the task, and the recording sites changed from session to session.

General data analysis

We analyzed the activity of 587 neurons with a stable response to the stimuli presented; details on the functional properties of these neurons are given in Merchant et al. (2001). A repeated-measures ANOVA was used to assess the statistical significance of the motion condition and location effects. The frequency of discharge (based on spike counts) during the last 300 ms of the 400-ms-long visual stimulation period was the dependent variable. The spike counts were square-root transformed to stabilize the variance (Snedecor and Cochran 1989). The activity of 150/587 (25.5%) cells that showed a significant main effect of motion condition and/or a significant effect of motion condition × location interaction was analyzed further in the tree clustering analyses in the following text.

The directional selectivity of cells to the translating dots was determined as follows. First, an ANOVA was performed, where the direction of translation was used as a factor. Then the directional tuning of these cells was assessed using bootstrap (Lurito et al. 1991) ($P < 0.05$).

Tree clustering analyses of stimulus motions

We performed tree clustering analyses to determine the pattern of grouping of 8 different kinds of stimulus motion using the activity of the 150 neurons in the preceding text. First, we defined the variables that served as the basis for cluster formation as follows. For each cell, the mean discharge rate for the eight motion conditions was calculated, by averaging the discharge rate during the last 300 of the 400 ms of visual motion stimulation across repetitions for those locations inside the receptive field mapped using a double Gaussian regression (Merchant et al. 2001). These values were standardized by re-expressing them as *z* scores that corresponded to the discharge rate variation of each motion condition around the mean of all motion conditions, expressed in SD units. Thus the primary clustering variables consisted of 150-dimensional vectors containing the *z* scores for each cell for every motion condition. The squared Euclidean distance between the 150-dimensional vectors of all possible pairs of motion conditions conformed an 8 × 8 dissimilarity matrix that was used in the tree clustering analyses described in the following text.

Two different analyses were performed on the dissimilarity matrix, namely an ultrametric and an additive tree analysis (Corter 1976). An ultrametric tree is a type of hierarchical clustering that can be fit by agglomerative algorithms and in which the path-length distances between clustering variables satisfy the following mathematical relationship for any three variables *a*–*c* in the tree

$$d(a, b) \leq d(a, c) = d(b, c)$$

where $d()$ corresponds to the distance between two variables. This equation that defines the ultrametric inequality, states that for every three variables *a*, *b* and *c*, *a* and *b* are less distant from each other than either is from *c*. This implies that *a* and *b* form a cluster relative to *c*. In the present study, the following agglomerative procedure was utilized for clustering. At the beginning of this procedure, all *N* motion conditions were considered as separate clusters. Then the pair of motion conditions closest to each other (i.e., the motion conditions

with the smallest Euclidean distance) was identified and combined to form a new cluster. The next step was to update the number clusters to $N - 1$ and to form the next cluster. This procedure was continued until all motion conditions were merged into one cluster. Finally, the method for combining clusters was the unweighted pair-group method using arithmetic averages that defines the distance between two clusters as the average of the distances between all pairs of cases in which one member of the pair is from each of the clusters (Johnson and Wichern 1998). The functions DCDIST and DCLINK of the IMSL library (Digital Visual Fortran, Professional Edition 1998) were used to execute the hierarchical tree clustering analysis. In the resulting trees (or dendrograms) horizontal distances represent estimated dissimilarities between motion conditions, whereas vertical distances are arbitrary.

We also used an additive tree analysis on the dissimilarity matrix to test for the robustness of clustering. An additive tree follows a basic mathematical relationship characterizing distances in the tree called additive inequality, and states that for any four variables in the tree that can be labeled as x, y, u and v

$$d(x, y) + d(u, v) \leq d(x, u) + d(y, v) = d(x, v) + d(y, u)$$

which implies that x, y form one cluster and u and v another. Additive trees are a more general structure, where the lengths of the leaf arcs are free to be of any length, whereas in ultrametric hierarchical trees all leaf nodes are equally distant from the root of the tree. The additive tree analysis was performed on the dissimilarity matrix using the program ADDTREE/P (ver. 1.05 by J.E. Corter 1981–1995). The overall goodness of additive tree clustering was assessed by the R^2.

Consense analysis

A hierarchical ultrametric clustering analysis of the different visual stimuli was also performed for each individual neuron. The 150 dendrograms obtained were analyzed using the program CONSENSE (version 3.5c by J. Felsenstein, University of Washington 1986–1993). This analysis provides the frequency of occurrence of the branch combinations in the population of dendrograms analyzed.

Tree clustering by different number of neurons

The minimum number of neurons necessary to produce the clustering observed in the dendrogram shown in Fig. 1 was computed using bootstrapping as follows. First, a fixed number of neurons K was chosen randomly with replacement. Then a hierarchical ultrametric clustering analysis was performed on the dissimilarity matrix for this group of neurons and the dendrogram structure saved. This procedure was repeated 1,000 times. Finally, two analyses were carried out on these 1,000 dendrograms. First, we counted the number (and percentage) of dendrograms that showed the same clustering of stimulus motions as in Fig. 1. And second, we performed a consensus analysis to estimate the robustness of specific clusters when smaller Ks were used.

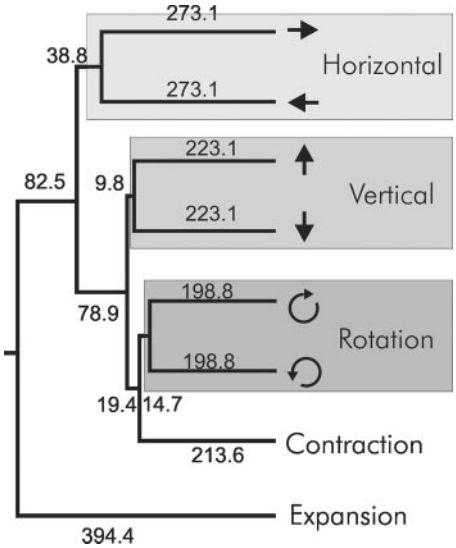

FIG. 1. *A*: dendrogram of the motion condition clustering derived from the normalized (z score) activity of 150 neurons using the hierarchical tree analysis method. The numbers within the dendrogram corresponds to the distance of each cluster in arbitrary units.

MDS analysis

The data for this analysis were the pairwise distances among the various clusters in the tree shown in Fig. 1. As mentioned in the preceding text, the distance between two clusters is the sum of the intervening horizontal distances; for example, the distance between the "horizontal" and "vertical" cluster is: 9.8 + 78.9 + 38.8 = 127.5 (arbitrary units) and so on for other pairs. The resulting dissimilarity matrix was analyzed by metric MDS, employing two dimensions and an interval scale (ALSCAL procedure, SPSS 10.1 for Windows, SPSS, Chicago, IL). The success of the MDS analysis was evaluated by computing Kruskal's stress formula 1 and the R^2. The latter is the proportion of variance of the scaled data (disparities) in the data which is accounted for by their corresponding distances. In addition, a plot of derived stimulus (i.e., tree clusters) configuration and a scatterplot of linear fit were generated.

RESULTS

The following results were obtained by analyzing the activity of 150 cells recorded in area 7a that showed a statistically significant effect of stimulus motion condition in an ANOVA (see METHODS). Although the presence of such an effect indicated a differential influence on cell activity of the various types of stimulus motion applied (i.e., right-, left-, up-, and downward, expansion, contraction, CW, and CCW) (see Merchant et al. 2001 for details), it did not, by itself, reveal any underlying orderly pattern of variation of neuronal activity with respect to the stimulus parameters. This issue was investigated in this study using tree clustering and MDS.

Tree-clustering analyses

Hierarchical (ultrametric) and an additive tree analyses were used to determine the clustering pattern of stimulus motions based on cell responses. The ultrametric dendrogram obtained is shown in Fig. 1. It can be seen that the two directions of horizontal motion (rightward and leftward), the two directions of vertical motion (upward and downward), and the two directions of rotatory motion (CW and CCW) were clustered in three separate branches (horizontal, vertical, and rotatory motion, respectively). In contrast, no such clustering was observed for the radial aspect of stimulus motion (expansion, contraction). In fact, contraction and expansion were in separate branches, and expansion was in its own branch by itself. It is worth mentioning that the same tree configuration was observed using additive tree analysis ($R^2 = 0.96$).

Tree clustering is a multivariate analysis that does not assign a probability value to the occurrence of different groupings. For that purpose, we used bootstrapping to compute the probability of obtaining by chance the entire population clustering (Fig. 1) and each of the major clusters. In this analysis, the z scores of the eight conditions were randomly permuted for

every cell, and a hierarchical tree clustering analysis performed on 150 bootstrapped cells. The results showed that the stimulus motion clustering of Fig. 1 was never observed on the total number of bootstraps ($n = 10^4$; hence $P < 10^{-4}$).

The clustering in Fig. 1 was not observed in the dendrogram derived from the population of those cells that did not show a significant stimulus motion effect in the ANOVA ($n = 217$; Fig. 2*A*) nor in the dendrogram produced from a population of cells recorded in motor cortex ($n = 108$; Fig. 2*B*) under identical stimulation conditions (Merchant et al. 2001). In addition, the clustering of opposite horizontal, vertical, and rotatory motions was not observed at the single cell level. An example from a single cell is shown in Fig. 3, *A* and *B*. Figure 3*C* shows that frequency of occurrence of each cluster or branch observed in the single cell analysis was >10% in most of the clusters.

Next we investigated the relation between the number *K* of neurons in the population and the probability of obtaining the clustering in the dendrogram observed. The results are shown in Fig. 4*C*, where is evident that the probability of obtaining the dendrogram observed (Fig. 1) increases with *K*, and essentially plateaus at $K \approx 130$ cells.

Robustness of branch clustering

It would be of interest to know the robustness of the clustering shown in Fig. 1. We assessed this issue by constructing consensus dendrograms generated by bootstrapping the actual data at different *K* values. Figure 4*A* shows examples of such dendrograms and *B* summarizes the outcome of this analysis as a plot of the probability of a cluster occurrence (left-right, up-down, CW-CCW, expansion alone), irrespective of other clusters, against *K*. It can be seen that this probability decreased with lower *K* values (as expected) for all clusters above. However, the rate of this decrease was smaller for the expansion alone and the right-left cluster than for the CW-CCW and up-down cluster. Therefore the former two groupings were more robust than the latter two.

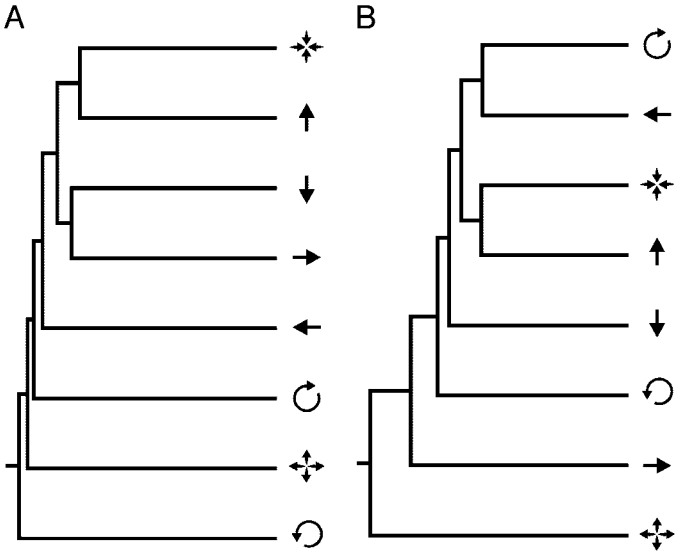

FIG. 2. *A*: dendrogram derived from normalized activity of 217 neurons in area 7a that did not showed significant effects in motion condition in the ANOVA using the hierarchical tree clustering analysis. *B*: dendrogram derived from normalized activity of 108 motor cortical neurons that showed a significant effect in motion condition.

MDS analysis

The MDS analysis was successfully applied on the tree-cluster dissimilarity matrix; the stress value was 0.026 and the R^2 was 0.998. The derived tree-cluster configuration plot and linear fit are shown in Fig. 5, *A* and *B*, respectively. It can be seen in Fig. 5*A* that the most important dimension (abscissa) separated expansion from all other stimulus motions, whereas the second dimension (ordinate) separated planar motions from motion in depth. The linear fit between the disparities (monotonically transformed data) versus the obtained distances is showed in Fig. 5*B*. This scatter plot represents the fit of the derived distances to the data, which is the fit that is being optimized by the MDS procedure. It is obvious that there is an almost perfect linear relation between these two measures, which was reflected in the high R^2 and the low stress value obtained.

DISCUSSION

In this study, we investigated the presence of a higher-order organization underlying the functional responses of posterior parietal neurons to basic optic-flow motions. This approach was motivated by three considerations. First, the stimulus motions we used, i.e., {right-, left-, up-, an downward}, {CW,CCW}, and {expansion, contraction}, are subordinate to the more general categories of planar motion, circular motion, and radial motion, respectively. Therefore it was reasonable to try to find out whether the latter superordinate aspects of optic flow could be represented at the level of the neuronal population. It should be noted that this analysis was not aimed to reconstruct the visual stimulus from the neuronal responses and has nothing to do with the population vector analysis employed to that end by other researchers in studies of visual motion (Kruse et al. 2002; Page and Duffy 1999; Steinmetz et al. 1987). The second consideration stems from behavioral aspects, namely the prominence of expansion in daily life due to locomotion. Locomotion is a common, if not the most common, activity of an organism, and during this activity, the dominant optic flow consists of expansion. Accordingly, we were interested in the possibility that expansion may be represented in a privileged way, so to speak, compared with the other kinds of visual motion. Finally, Shepard's instrumental work on deriving hidden principles of organization from proximity (i.e., similarity or dissimilarity) judgments using tree clustering and MDS (Shepard 1980) led us to the use of the very same methods to analyze neural response data for the purpose of uncovering latent organizational principles in the visual motion domain. In fact, our application of these analyses followed closely that of Shepard's in using both of the aforementioned methods to gain complementary insights into this organization. Indeed, both analyses provided excellent fit to the data ($R^2 = 0.96$ and 0.998 for the additive tree clustering and MDS, respectively) and their results are discussed separately in the following text.

The tree-clustering analysis revealed a grouping of opposite basic directions of motion into superordinate units. Thus left-/rightward stimuli were grouped together, as well as up-/downward and CW/CCW. The interpretation of these superordinate units is obvious as they signify horizontal, vertical, and rotatory motions, respectively. This clustering

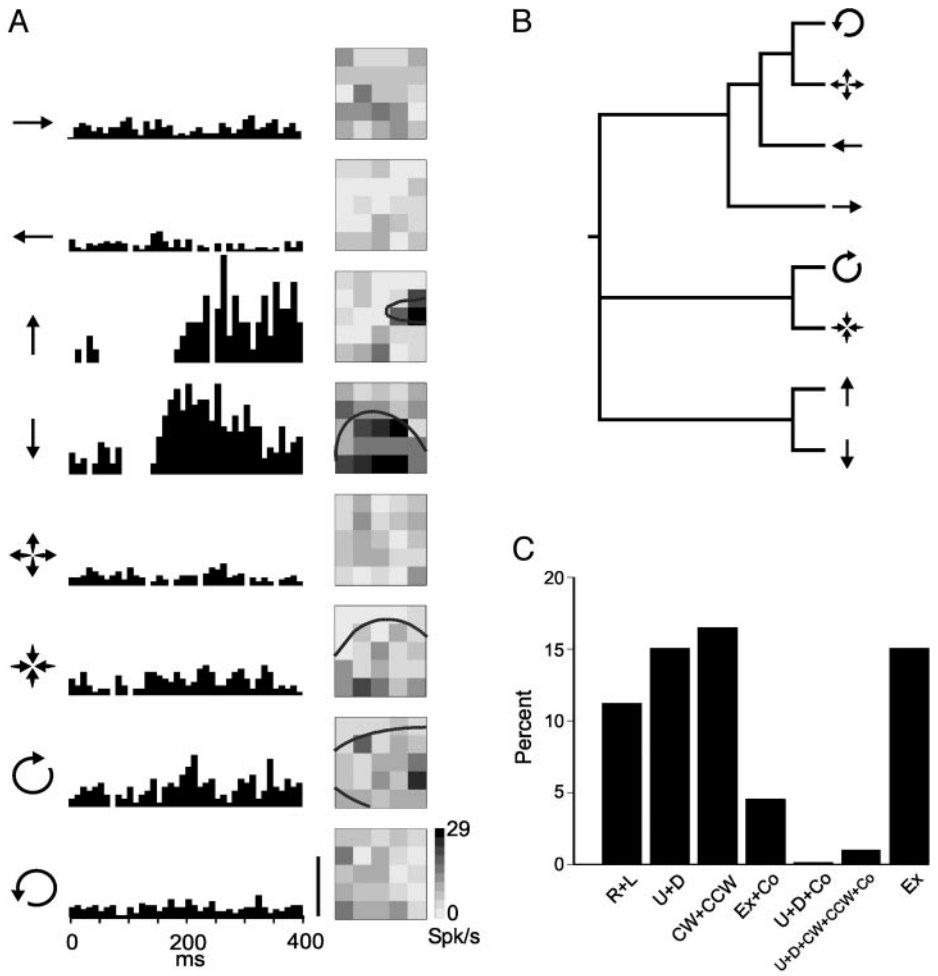

FIG. 3. Data and analyses for a single cell. *A*: peristimulus time histogram (*left*) and gray-scale response graphs including the receptive fields (*right*) for the stimulus motion conditions shown to the left. *B*: dendrogram derived from these data. *C*: frequency of occurrence of the noted clusters in the population of 150 single-cell dendrograms derived, 1 for each cell. R, rightward; L, leftward; U, upward; D, downward; CW, clockwise; CCW, counterclockwise; Ex, expansion; Co, contraction.

of opposite directions may appear to be counter intuitive from the viewpoint of cell tuning to stimulus direction. For example, if cells were tuned to the direction of dot translation, one would expect the resulting dendrogram configuration to be such that opposite directions (i.e., the preferred and its opposite) would be in separate branches, but this was not observed in our study. We believe that this is due to the fact that only 29 of the150 cells (19.3%) included in the hierarchical tree-clustering analysis were significantly tuned to rectilinear stimulus motion. Although the horizontal, vertical, and rotatory motions were represented individually at the single cell level, the simultaneous grouping of these three motion classes apparently is an emergent property (Johnson 2000) of the neuronal ensemble because it was not observed at the single-cell level. This higher-order organization of functional cell properties complements previous observations on area 7a cellular responses to moving stimuli in general (Motter and Mountcastle 1981; Sakata et al. 1994; Steinmetz et al. 1987) as well as to optic-flow stimuli in particular (Read and Siegel 1997; Siegel and Read 1997). It should be mentioned that the tree-clustering analyses aim to identify groups in a multivariate set of data (Shepard 1980). These analyses are based on similarities (or dissimilarities) between the objects, and no assumptions are made concerning the number of groups or group structure that can be obtained (Johnson and Wichern 1998). Thus the fact that the horizontal, vertical, and rotation types of stimulus motion were grouped together in the present results was not due to a priori considerations in the analyses. Therefore this dendrogram configuration depends on the multivariate relationships between the firing rates of the population of area 7a neurons during the presentation of the different types of stimulus motion. Finally, it should be noted that in this study, stimuli were delivered in patches of the visual field; possible responses to full-flow stimulation were not investigated.

The findings in the preceding text do not necessarily follow from the existence of a selectivity of single-cell discharge to optic flow. This is evidenced by the fact that such selectivity was also observed in the motor cortex (Merchant et al. 2001) but no clustering was found in that area (Fig. 2*B*). The clustering in the preceding text does not necessarily follows from the existence of a selectivity of single-cell discharge to optic flow because such selectivity was also observed in the motor cortex (Merchant et al. 2001) but no clustering was found in that area (Fig. 2*B*). Therefore the clustering observed in area 7a seems to rely on specific constraints among cell responses to the different kinds of optic-flow stimuli. Apparently, such constraints are absent in the motor cortex, and there may or may be not present in other areas, such as MST. Although the nature of these putative constraints is not known, one could speculate on the substrate that would be necessary for them to operate on. Obviously, this should be a substrate of diverse responses by

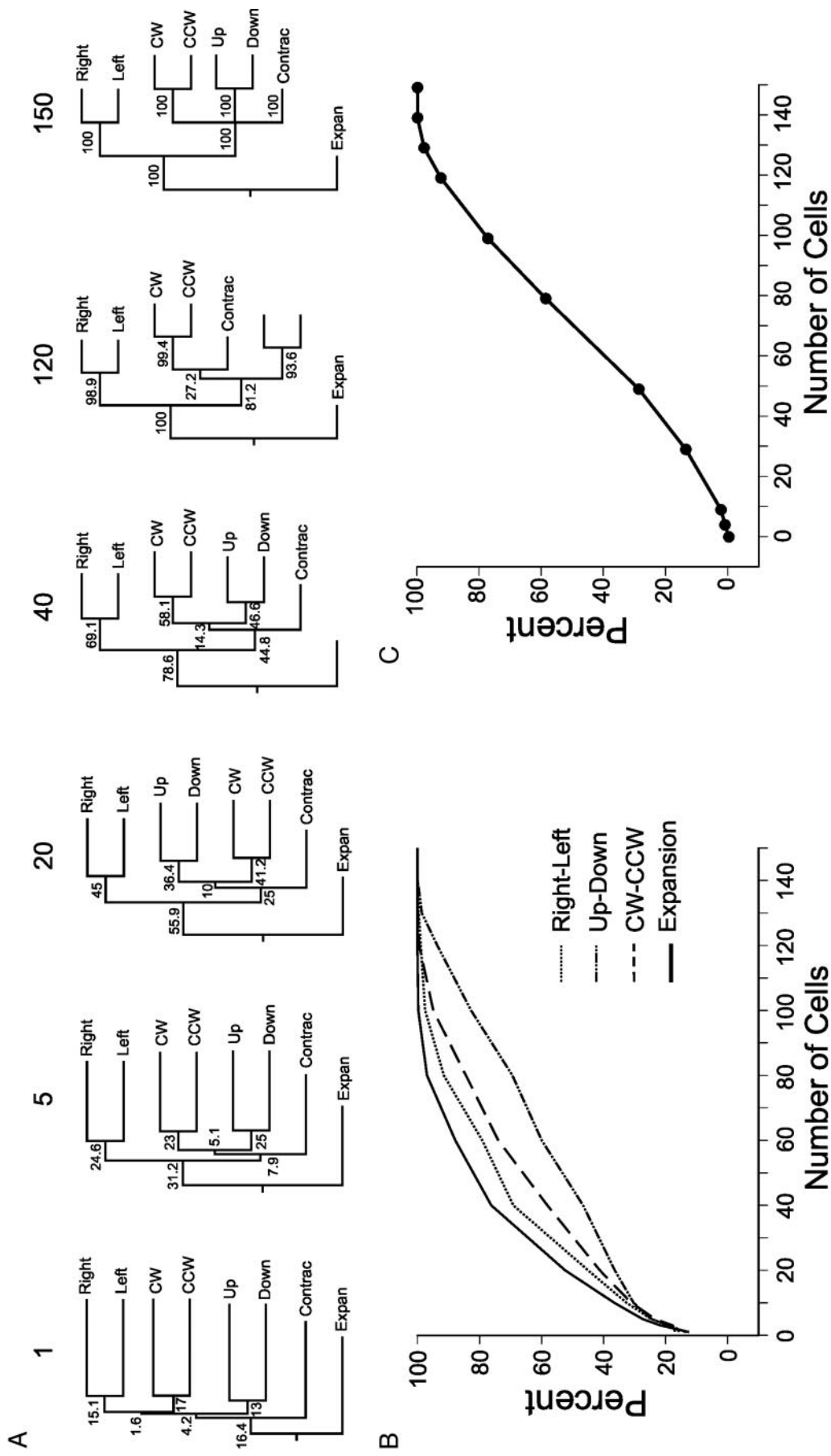

FIG. 4. *A*: consensus dendrograms for selected numbers *K* of contributing neurons, noted above each dendrogram. Each dendrogram is the consensus dendrogram derived from 1,000 bootstrap samples. Numbers within a dendrogram indicate the percentage of times in which the particular branch (cluster) was observed. *B*: percentages of occurrence of the 4 branches noted are plotted against *K*. *C*: percent of times that the clustering in the dendrogram of Fig. 1 was obtained from different numbers of contributing cells (abscissa).

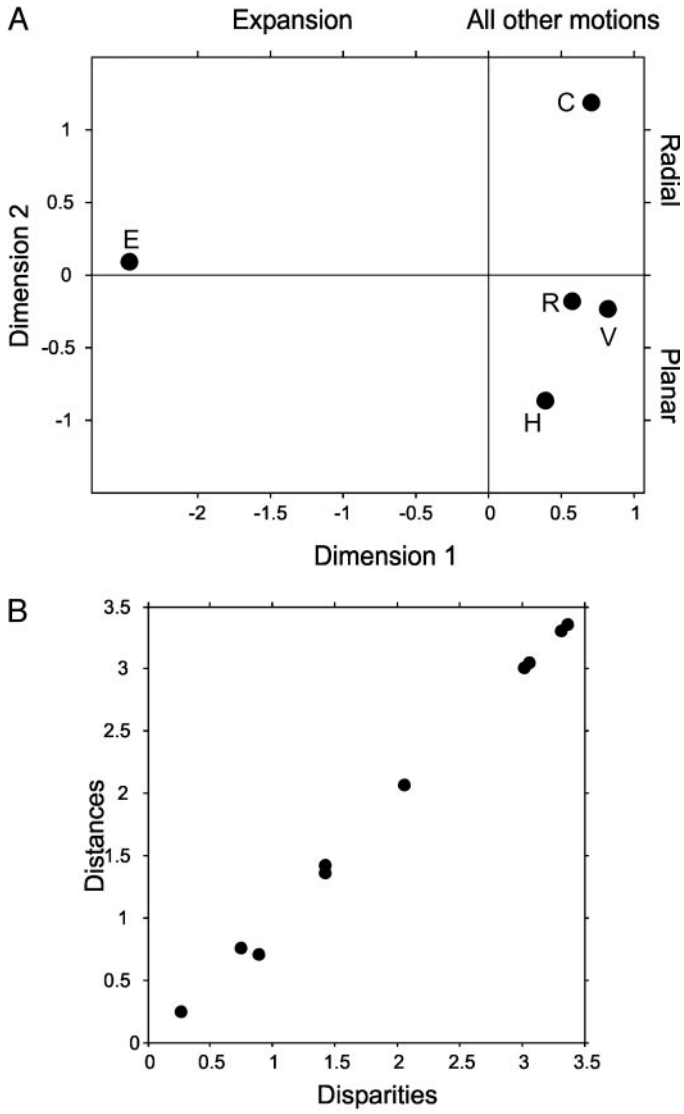

FIG. 5. Results of the multidimensional scaling (MDS) analysis. *A*: 2-dimensional representation of the 5 superordinate clusters in the tree-clustering analysis. H, horizontal; V, vertical; R, rotation, E, expansion; C, contraction. *B*: scatter plot of linear fit between the disparities (monotonically transformed data) vs. the distances. This plot displays the small amount of departure from linearity, which is directly related with the obtained high R^2 (0.998) and low stress value (0.026).

single cells to a variety of optic-flow stimuli. It is noteworthy that this clustering was present in small cell ensembles (Fig. 4), which indicates that the underlying conditions for the clustering are widely distributed in the population.

The clustering of vertical and horizontal axis by cells in area 7a could relate to different aspects of depth perception, including perception of motion in depth, perception of change in the size of an object, and the visual guidance of locomotion. The results of psychophysical experiments (Beverly and Regan 1979; Regan and Gray 2000) have suggested that the presence of one-dimensional relative motion subsystems is necessary to perceive motion in depth or the change in size of an object; these subsystems integrate the input from opposing directionally selective neurons, the output of which signals the speed and sign of relative motion of the object along a given retinal meridian. Our results suggest that cells in area 7a could be the part of this relative motion subsystem. In contrast to the clustering of planar motions, radial motions were split: expansion was all by itself, whereas contraction was alone but within a larger cluster comprising the planar motions (Fig. 1). This finding suggests that radial motion, and, within it, expansion and contraction, are represented quite differently in the ensemble. Specifically, the fact that expansion was in a branch stemming directly off the root of the dendrogram indicates a fundamental difference between expansion and all other stimulus motions. This special place of expansion may stem from the fact that it is perhaps the most frequently generated kind of stimulus motion in species with forward locomotion: its high frequency of occurrence in daily life may account for its uniqueness in the population coding of stimulus motion but also for its high prevalence as a major effect on the activity of cells in various cortical areas (Anderson and Siegel 1999; Duffy and Wurtz 1991; Schaafsma and Duysens 1996; Siegel and Read 1997). It is possible that the planar optic flow that accompanies locomotion may be principally relevant to maintaining dynamic stability while locomoting and accordingly is located on the other main branch of the hierarchy in the observed clustering (Fig. 1).

These considerations and interpretations of the tree-clustering results were further supported by the results of the MDS analysis. We used MDS as a second stage of analysis to gain an insight into the dimensions along which the tree clusters varied; therefore the data used as input to the MDS analysis were the derived inter-cluster distances (Fig. 1). The results obtained indicated two dimensions in operation (Fig. 5*A*). The first dimension separated expansion from all other stimuli; this underscores the uniqueness of this kind stimulus motion and probably signifies its importance for locomotion. This dimension could have been inferred from the tree-clustering analysis as evidenced by the placement of the expansion and all other stimulus motions combined in two separate clusters. Now, the second dimension in MDS obviously separated planar from radial motions, a finding not apparent in the tree-clustering analysis. A possible interpretation of the grouping of up-down, left-right, and CW/CCW motions is that all of them correspond to rotations with respect to the three cardinal axes of rotation. For example, to a good approximation, the up-down motions could come from rotation of the eyes or head-plus-eyes about a pitch axis through the head, the left-right motion could come from rotation of the eyes or head-plus-eyes about a yaw axis through the head, and the CW/CCW rotation could come from rotation of the eyes or head-plus-eyes about a roll axis through the head. In addition, the up-down and left-right motions could also come from up-down and left-right translatory movement of the head, respectively. In contrast to these considerations, radial motions can only come from translation in depth, which, in turn, typically comes about from moving in space, a very common activity. We believe that it is this last feature that is captured by the second dimension in the MDS plot (Fig. 5*A*). Thus radial motion in general, and expansion in particular, seem to hold a special place in the ensemble processing of visual motion in area 7a, reflecting, most probably, behavioral considerations.

DISCLOSURES

This work was supported by National Institute of Mental Healt Grant PSMH-48185, the United States Department of Veterans Affairs, and the American Legion Brain Sciences Chair.

REFERENCES

Albright TD. Direction and orientation selectivity of neurons in visual area MT of the macaque. *J Neurophysiol* 52: 1106–1130, 1984.

Andersen RA. Neural mechanisms of visual motion perception in primates. *Neuron* 18: 865–872, 1997.

Andersen RA, Asanuma C, Essick G, and Siegel RM. Corticocortical connections of anatomically and physiologically defined subdivisions within the inferior parietal lobule. *J Comp Neurol* 296: 65–113, 1990.

Anderson KC and Siegel RM. Optic flow selectivity in the anterior superior temporal polysensory area, STPa, of the behaving monkey. *J Neurosci* 19: 2681–2692, 1999.

Beverly KI and Regan D. Separable aftereffects of changing-size and motion-in-depth: different neural mechanisms? *Vis Res* 19: 727–732, 1979.

Boussaoud D, Ungerleider LG, and Desimone R. Pathways for motion analysis: cortical connections of the medial superior temporal and fundus of the superior temporal visual areas in the macaque. *J Comp Neurol* 296: 462–495, 1990.

Bruce C, Desimone R, and Gross CG. Visual properties of neurons in a polysensory area in superior temporal sulcus of the macaque. *J Neurophysiol* 46: 369–384, 1981.

Cavada C and Goldman-Rakic PS. Posterior parietal cortex in the rhesus monkey. I. Parcellation of areas based on distinctive limbic and sensory corticocortical connections. *J Comp Neurol* 287: 393–421, 1989.

Cheng K, Fujita H, Kanno I, Miura S, and Tanaka K. Human cortical regions activated by wide-field visual motion: an H2(15)O PET study. *J Neurophysiol* 74: 413–427, 1995.

Colby CL, Duhamel JR, and Goldberg ME. Ventral intraparietal area of the macaque: anatomic location and visual response properties. *J Neurophysiol* 69: 902–914, 1993.

Corter JE. *Tree Models of Similarity and Association.* Thousand Oaks, CA: SAGE, 1976.

Duffy CJ and Wurtz RH. Sensitivity of MST neurons to optic flow stimuli. I. A continuum of response selectivity to large-field stimuli. *J Neurophysiol* 65: 1329–1345, 1991.

Johnson NL. Importance of diversity. Reconciling natural selection and non-competitive processes. *Ann NY Acad Sci* 901: 54–66, 2000.

Johnson RA and Wichern DW. *Applied Multivariate Statistical Analysis.* Englewood Cliffs, NJ: Prentice Hall, 1998.

Koenderink JJ. Optic flow. *Vis Res* 26: 161–180, 1986.

Kruse W, Dannenberg S, Kleiser R, and Hoffmann KP. Temporal relation of population activity in visual areas MT/MST and in primary motor cortex during visually guided tracking movements. *Cereb Cortex* 12: 466–476, 2002.

Lagae L, Maes H, Raiguel S, Xiao DK, and Orban GA. Responses of macaque STS neurons to optic flow components: a comparison of areas MT and MST. *J Neurophysiol* 71: 1597–1626, 1994.

Lee DN. A theory of visual control of braking based on information about time-to-collision. *Perception* 5: 437–459, 1976.

Lee DN. The optic flow field: the foundation of vision. *Philos Trans R Soc Lond B Biol Sci* 290: 169–179, 1980.

Lurito JT, Georgakopoulos T, and Georgopoulos AP Cognitive spatial-motor processes. VII. The making of movements at an angle from a stimulus direction: studies of motor cortical activity at the single cell and population levels. *Exp Brain Res* 87: 562–580, 1991.

Merchant H, Battaglia-Mayer A, and Georgopoulos AP. Effects of optic flow in motor cortex and area 7a. *J Neurophysiol* 87: 1937–1954, 2001.

Motter BC and Mountcastle VB. The functional properties of the light-sensitive neurons of the posterior parietal cortex studied in waking monkeys: foveal sparing and opponent vector organization. *J Neurosci* 1: 3–26, 1981.

Newsome WT, Britten KH, Salzman CD, and Movshon JA. Neuronal mechanisms of motion perception. *Cold Spring Harb Symp Quant Biol* 55: 697–705, 1990.

Oram MW, Perrett DI, and Hietanen JK. Directional tuning of motion-sensitive cells in the anterior superior temporal polysensory area of the macaque. *Exp Brain Res* 97: 274–294, 1993.

Page WK and Duffy CJ. MST neuronal responses to heading direction during pursuit eye movements. *J Neurophysiol* 81: 596–610, 1999.

Read HL and Siegel RM. Modulation of responses to optic flow in area 7a by retinotopic and oculomotor cues in monkey. *Cereb Cortex* 7: 647–661, 1997.

Regan D and Gray R. Visually guided collision avoidance and collision achievement. *Trends Cogn Sci* 4: 99–107, 2000.

Sakata H, Shibutani H, Ito Y, Tsurugai K, Mine S, and Kusunoki M. Functional properties of rotation-sensitive neurons in the posterior parietal association cortex of the monkey. *Exp Brain Res* 101: 183–202, 1994.

Salzman CD, Britten KH, and Newsome WT. Cortical microstimulation influences perceptual judgements of motion direction. *Nature* 346: 174–177, 1990.

Salzman CD, Murasugi CM, Britten KH, and Newsome WT. Microstimulation in visual area MT: effects on direction discrimination performance. *J Neurosci* 12: 2331–2355, 1992.

Schaafsma SJ and Duysens J. Neurons in the ventral intraparietal area of awake macaque monkey closely resemble neurons in the dorsal part on the medial superior temporal area in their responses to optic flow patterns. *J Neurophysiol* 76: 4056–4068, 1996.

Shepard RN. Multidimensional scaling, tree-fitting, and clustering. *Science* 210: 390–398, 1980.

Siegel RM and Read HL. Analysis of optic flow in the monkey parietal area 7a. *Cereb Cortex* 7: 327–46, 1997.

Snedecor GW and Cochran WG. *Statistical Methods.* Ames, IA: Iowa State University Press, 1989.

Steinmetz MA, Motter BC, Duffy CJ, and Mountcastle VM. Functional properties of parietal visual neurons: radial organization of directionalities within the visual field. *J Neurosci* 7: 177–191, 1987.

Tanaka K, Hikosaka K, Saito H, Yukie M, Fukada Y, and Iwai E. Analysis of local and wide-field movements in the superior temporal visual areas of the macaque monkey. *J Neurosci* 6: 134–144, 1986.

Tanaka K and Saito HA. Analysis of motion of the visual field by direction, expansion/contraction, and rotation cells clustered in the dorsal part of the medial superior temporal area of the macaque monkey. *J Neurophysiol* 62: 626–641, 1989.

Tootell RB, Reppas JB, Kwong KK, Malach R, Born RT, Brady TJ, Rosen BR, and Belliveau JW. Functional analysis of human MT and related visual cortical areas using magnetic resonance imaging. *J Neurosci* 15: 3215–3230, 1995.

Van Essen DC, Maunsell JH, and Bixby JL. The middle temporal visual area in the macaque: myeloarchitecture, connections, functional properties and topographic organization. *J Comp Neurol* 199: 293–326, 1981.

Zeki SM. Functional organization of a visual area in the posterior bank of the superior temporal sulcus of the rhesus monkey. *J Physiol* 236: 549–573, 1974.

Zeki S, Watson JD, Lueck CJ, Friston KJ, Kennard C, and Frackowiak RS. A direct demonstration of functional specialization in human visual cortex. *J Neurosci* 11: 641–649, 1991.